



Research Article

# Comparison the start-up time of the key parameters of aqua-ammonia and water–lithium bromide absorption chiller (AC) under different heat exchanger configurations

Abolfazl Ebrahimmataj Tiji<sup>1</sup> · Abas Ramiar<sup>2</sup> · Mohammadreza Ebrahimmataj<sup>3</sup>

Received: 1 December 2019 / Accepted: 28 July 2020 / Published online: 17 August 2020  
© Springer Nature Switzerland AG 2020

## Abstract

The time that an absorption chiller needs to reach the designed working condition is called start-up. During this time, energy is consumed through the system while efficient refrigeration is not available. So, it's too important to consider the influencing parameters on this period of time so that reduction in energy consumption is achieved. Also, dynamic analysis is used to reduce the startup time and increase system performance in addition to strategic control purposes. Optimizing an absorption cycle during transient operations, such as start up or shut down is very important. The aim of this study is to investigate and compare the effect of employing refrigerant and solution heat exchangers (RHX and SHX) on dynamic performance of both NH<sub>3</sub>–H<sub>2</sub>O and H<sub>2</sub>O–LiBr absorption chillers (ACs). Also, the effect of solution heat exchanger's efficiency on the start-up time of the key parameters of both ACs is investigated. To diminish the effect of approximate relations on the results, thermodynamic properties of NH<sub>3</sub>–H<sub>2</sub>O and H<sub>2</sub>O–LiBr solutions are extracted from the EES software. By making a link between MATLAB and EES software, a set of differential equations is solved in MATLAB software. The fourth order Runge–Kutta method is employed to solve the differential equations system. This process is continued until convergence criteria are satisfied. The results show that removing SHX from the cycle increases the start-up time of both NH<sub>3</sub>–H<sub>2</sub>O and H<sub>2</sub>O–LiBr AC's COPs by 11.76% and 45.16% respectively. The start-up time of the COP of H<sub>2</sub>O–LiBr absorption chiller is highly affected in comparison with the NH<sub>3</sub>–H<sub>2</sub>O absorption cycle, by removing SHX or increasing the SHX efficiency. Also, utilizing the RHX does not affect the dynamic response of the key parameters of the both absorption chillers.

**Keywords** Transient simulation · Refrigerant and solution heat exchangers · Aqua-ammonia · Water–lithium bromide · Start-up time · Absorption chiller

## List of symbols

A	The pipe cross-sectional area (m <sup>2</sup> )	<i>LMTD</i>	The logarithmic mean temperature difference (K)
COP	Coefficient of performance	<i>M</i>	Mass (kg)
<i>c<sub>p</sub></i>	Specific heat at constant pressure (kJ/kg K)	<i>m</i>	Mass flow rate between components (kg/s)
<i>d</i>	Pipe diameter (m)	<i>P</i>	Pressure (kg/m s <sup>2</sup> )
<i>h</i>	Specific enthalpy (kJ/kg)	<i>Q̇</i>	Heat transfer rate (kW)
<i>L</i>	Pipe length (m)	<i>T</i>	Temperature (°C)
		<i>t</i>	Time (s)

✉ Abolfazl Ebrahimmataj Tiji, a\_nataj@semnan.ac.ir | <sup>1</sup>Department of Mechanical Engineering, Semnan University, Semnan, Iran. <sup>2</sup>Faculty of Mechanical Engineering, Babol Noshirvani University of Technology, Babol, Iran. <sup>3</sup>Department of Mechanical Engineering, Qom University of Technology, Qom, Iran.



$UA$	Conductance (kW/K)
$V$	Volume ( $m^3$ )
$X$	Concentration of ammonia–water solution at the absorber and generator
$XI$	Concentration of water–lithium bromide solution at the exit of generator and absorber
$Z$	Concentration of water–lithium bromide solution at the absorber and generator
Start-up time	The time required for each parameter to reach steady state condition
$Qu$	Quality

**Greek letters**

$\varepsilon$	Efficiency of the solution heat exchanger
$\xi$	The expansion valve friction factor
$\rho$	Density ( $kg/m^3$ )

**Subscripts**

a, A	Absorber
c, C	Condenser
e, E	Evaporator
g, G	Generator
p	Pump

**Abbreviations**

SHX	Solution heat exchanger
RHX	Refrigerant heat exchanger or (condensate pre-cooler)
AC	Absorption chiller
EES	Engineering equation solver

## 1 Introduction

Chillers are among the most important cooling equipment that can generally be divided into two categories of compression and absorption chillers. Absorption chillers are classified in two types; water–lithium bromide cycle in which water is considered as a refrigerant and lithium bromide as an absorbent, and ammonia–water cycle whose refrigerant is ammonia and absorbent is water. Compression chillers use electrical energy while absorption chillers use thermal energy as an energy alternative to produce cooling. Absorption chillers have two main superiorities when they are compared with the compression chillers which are; the use of renewable energy as an input alternative such as solar energy, geothermal and heat lost from industrial processes, and their compatibility with the environment [1, 2]. Nowadays, environmental concerns about ozone depletion and global warming, on the one hand, and surplus energy consumption, rising fuel prices, etc., on the other hand, have made the absorption chillers more attractive to researchers. Absorption chillers are very

suitable tools for reducing electric energy consumption and recovering waste heat from industrial plants [1–4]. Simulations are way very important tools for researchers to predict the performance of absorption chillers at the dynamic level with low cost. Coupling any renewable energy device to the chiller is easily performed without any cost.

Many papers have been so far published in the field of dynamic simulation of absorption refrigeration systems. Kohlenbach and Ziegler [5, 6] presented dynamic simulation of the water–lithium bromide absorption chiller based on external and internal steady-state enthalpy balances for each main component. Dynamic behavior of the model was described by mass storage terms in the absorber and generator, thermal heat storage terms in all vessels and a time-delay in the solution cycle. Many researchers conducted dynamic model of the absorption cycle by using the mass and energy conservation and momentum equations [7–11]. Investigation the behavior of the absorption cycle in dynamic mode by applying the step change in the cycle [5, 6, 8, 12, 13] and during start-up [7, 14, 15] have been already carried out. Dynamic simulation of ammonia–water heat pump [8, 16–19] was accomplished to predict the transient performance and design characteristics as well.

Some researchers have presented dynamic model for absorption chillers by using TRNSYS software and Simulink environment [10, 13, 15, 17, 19–21]. Altun and Kilic [20] developed a dynamic model for a 10 KW cooling capacity solar-assisted absorption cycle for different cities of Turkey by TRNSYS software. They conducted a parametric study to investigation the effect of various parameters such as solar collector type, area, storage tank volume, collector slope, boiler set point temperature, room thermostat set point temperature on system efficiency. Their results show that in terms of financial analysis, Izmir is the most suitable city for solar-based absorption cooling system applications with a payback period of 10.7 years. Utilization of the exhaust waste heat of the internal combustion engines for the cooling systems input energy has been done by Wang et al. [21]. They developed dynamic simulation for 3 different cascade waste heat recovery systems listed as an electric-cooling cogeneration system (ECCS), a double-effect absorption refrigeration system, and a double-stage organic Rankine cycle. Also, dynamic response and off-design performance of three aforementioned cases were analyzed and compared. They presented validated module library for building different dynamic models in Simulink and validated by basic thermodynamic cycles.

Arora and Kaushik [22] conducted an energy and exergy analysis of single-effect and double-effect water–lithium bromide absorption cycle in order to examine the effect of heat exchanger efficiency and

component's temperature on some parameters such as; performance coefficient, rate of exergy destruction, and rate of exergy loss. Their analysis relied on the first and second law of thermodynamics using the mass and energy balance for each component. The EES software was applied to solve governing equation. They found that the maximum COP occurs at high generator temperature, and its rise is tied by evaporator temperature and increase in heat exchanger's efficiency as well. Sozen [23] studied the effect of heat exchanger on the aqua-ammonia absorption chiller's performance. More to the point, he studied the thermodynamic performance of absorption cycle and the irreversibility of the thermal process for different modes. Parameters such as COP, ECOP, circulation ratio and non-dimensional exergy loss are calculated separately for each component. The concentration of ammonia vapor at the rectifier outlet was set to constant value of 0.999. Later on, Kaynakli and Kilic [24] scrutinized the effect of refrigerant and solution heat exchangers on cycle performance, efficiency ratio and operating temperature. And, the effect of operating temperature and efficiency of heat exchanger on the thermal loads of components, coefficients of performance were also investigated. Their results revealed that the solution heat exchanger could increase the COP value by 44% as well as raising the refrigerant heat exchanger performance by 2.8%. Karamangil et al. [25] studied the thermodynamic analysis of single-effect absorption cycles with different working fluid pairs. Moreover, the influence of operating temperature, refrigerant, solution and solution-refrigerant heat exchanger efficiency on system performance were investigated. They concluded that the solution heat exchanger causes significant increase in the absorption cycle COP and its percentage stands at 66%, and in case of solution-refrigerant and refrigerant heat exchanger, this percentage reaches at 14% and 6%, respectively.

Previous studies [16–18, 26] only concentrated on the dynamic response under a single working condition. They have not taken into account the issue that how long it takes for a system to reach a new steady-state condition when system conditions change. Also, researchers, Refs. [22–25], studied the effect of refrigerant and solution heat exchangers and heat exchanger's efficiency on the performance of the absorption cycle in the steady state mode while dynamic mode still needs to be investigated. In our previous study, we investigated the effect of sub-cool liquid at condenser/absorber outlet and also, effect of ambient temperature on AC's key parameters launch time [11]. The general structure and some of input data and initial values of the previous and current research are similar, but the subject that, investigated in this article is different. The main goal of this article is to comparison the

start-up time of the key parameters of aqua-ammonia and water–lithium bromide absorption chiller under different heat exchanger configurations.

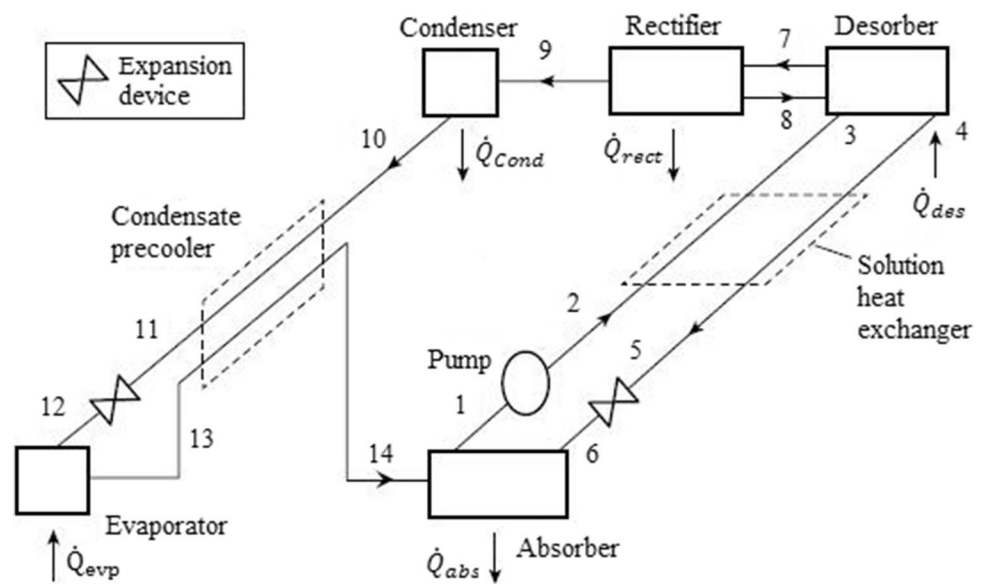
In this study, the thermodynamic analysis of the both  $\text{NH}_3\text{-H}_2\text{O}$  and  $\text{H}_2\text{O-LiBr}$  absorption refrigeration cycle is performed by applying the mass and energy balance, continuity of solution species and momentum equations. The performance of  $\text{NH}_3\text{-H}_2\text{O}$  and  $\text{H}_2\text{O-LiBr}$  absorption chillers is compared under different condition, which is not found in the literature. In fact, the aim of this study is to investigate and compare the start-up behavior of  $\text{NH}_3\text{-H}_2\text{O}$  and  $\text{H}_2\text{O-LiBr}$  absorption chillers by lumped parameter model under three different cases including; (1) utilizing RHX with SHX in the cycle, (2) removing RHX from the cycle, just SHX plays role in the cycle and (3) removing SHX from the cycle, just RHX plays role in the cycle. Also, the effect of solution heat exchanger's efficiency on the start-up time of the key parameters of the both ACs is studied and compared. Many researches employed polynomial functions approximation [13, 27–29] and EES software [9, 22] to extract the thermodynamic properties of  $\text{H}_2\text{O-LiBr}$  solution, and some of them [7, 14, 16, 19, 30] benefited from empirical relations and equations of state to estimate the thermodynamic properties of  $\text{NH}_3\text{-H}_2\text{O}$  solution. In this paper, in order to minimize the deviations resulted from approximated equations, the Engineering Equation Solver (EES) software is used to obtain the thermodynamic properties of the working fluids, and MATLAB software is employed to solve differential equations by fourth order Rung-Kutta method. EES and MATLAB software are linked by an Excel file. To validate dynamic model, the results obtained from this work are compared with the results of the steady state.

## 2 Dynamic modeling of the system

### 2.1 Governing equation

Figure 1 shows the schematic of the ammonia–water and water–lithium bromide absorption refrigeration cycle with the refrigerant and solution heat exchangers. The main components of the absorption refrigeration cycle are as follows; evaporator, absorber, generator, condenser, pump, refrigerant and solution heat exchangers. The refrigerant and solution heat exchangers are two important devices in absorption refrigeration cycles. The solution heat exchanger heats the cool solution from the absorber on the way to the generator and cools down the solution returning from the generator to the absorber. Thus, the heat load decreases in the generator and the COP increases. In the refrigerant heat exchanger (condensate pre-cooler), which is in the refrigeration side of the cycle, the refrigerant leaving the condenser is cooled by the vapor coming from the evaporator, and the

**Fig. 1** Schematic of absorption refrigeration cycle with both SHX and RHX (condensate pre-cooler) [31]



enthalpy of the liquid decreases. Since the cooling capacity increases, the COP value increases [24].

The following assumptions are made to simplify the simulation were clearly stated in the literature:

- Concentration of ammonia vapor at the generator outlet is considered at its constant value of 0.9996 [31, 32].
- Refrigerant leaves the generator at the state of saturated vapor [9–11, 27, 28, 31].
- Refrigerant leaving the evaporator and condenser is at the state of saturated vapor and saturated liquid respectively [9–11, 27, 28, 31].
- Fluid outlet temperature from each single component is equaled to inside temperature of its component [9–11, 27, 28].
- The amount of work given to the pump is negligible [9–11].
- There is no pressure loss in the pipes [9, 11].

In this study, each component of the absorption cycle is considered as a control volume. Mass, energy balance and momentum equations are used for dynamic analysis. As labeled in Fig. 1,  $M_i(t)$  corresponds to the mass within component  $i$ , and  $\dot{m}_i(t)$  indicates the mass flow rate between components. Subsequently, the overall mass balances for each component are formed by [9, 11]:

$$\frac{d}{dt}(M_C) = \dot{m}_7 - \dot{m}_8 \quad (1)$$

$$\frac{d}{dt}(M_E) = \dot{m}_8 - \dot{m}_{10} \quad (2)$$

$$\frac{d}{dt}(M_A) = \dot{m}_{10} + \dot{m}_6 - \dot{m}_1 \quad (3)$$

$$\frac{d}{dt}(M_G) = \dot{m}_1 - \dot{m}_6 - \dot{m}_7 \quad (4)$$

$$\dot{m}_1 = \dot{m}_2 = \dot{m}_3 \quad (5)$$

$$\dot{m}_4 = \dot{m}_5 = \dot{m}_6 \quad (6)$$

$$\dot{m}_8 = \dot{m}_9 \quad (7)$$

For aqua-ammonia absorption cycle,  $X_i(t)$  is the mass fraction of the ammonia in the component. Subsequently, we have the following absorbent mass balances in the absorber and generator [8, 11]:

$$\frac{d}{dt}(X_A) = \left(\frac{1}{M_A}\right) [\dot{m}_{10}X_7 + \dot{m}_6X_G - \dot{m}_1X_A - X_A(\dot{m}_{10} + \dot{m}_6 - \dot{m}_1)] \quad (8)$$

$$\frac{d}{dt}(X_G) = \left(\frac{1}{M_G}\right) [\dot{m}_1X_A - \dot{m}_6X_G - \dot{m}_7X_7 - X_G(\dot{m}_1 - \dot{m}_6 - \dot{m}_7)] \quad (9)$$

$$X_A = X_1 = X_2 = X_3 \quad (10)$$

$$X_G = X_4 = X_5 = X_6 \quad (11)$$

For water–lithium bromide absorption cycle,  $Z_i$  stands for the concentration of  $H_2O$ –LiBr solution in the absorber and generator. The concentration of solution at the generator and absorber outlet is indicated by  $x_l$  [9].

$$\frac{d}{dt}(Z_A) = \left(\frac{1}{M_A}\right) [\dot{m}_6 x_{L_G} - \dot{m}_1 x_{L_A} - Z_A(\dot{m}_{10} + \dot{m}_6 - \dot{m}_1)] \tag{12}$$

$$\frac{d}{dt}(Z_G) = \left(\frac{1}{M_g}\right) [\dot{m}_1 x_{L_A} - \dot{m}_6 x_{L_G} - Z_G(\dot{m}_1 - \dot{m}_6 - \dot{m}_7)] \tag{13}$$

The concentration of solution at the exit of generator and absorber in LiBr–H<sub>2</sub>O absorption chiller is a function of the quality and solution concentration of generator and absorber respectively. The concentrations of solution at the generator and absorber were not assumed to be equal to the corresponding concentration at the exit of those components. The relationship between concentration of solution at the exit of generator and absorber, quality and concentration of solution in components are followed by [9]:

$$z_i = x_{Li}(1 - Qu_i) \tag{14}$$

As the quality approaches to zero, the amount of Z will become equal to XI. This effect is neglected in the NH<sub>3</sub>–H<sub>2</sub>O absorption chiller [9].

The momentum equations between the components are given by [8–11]:

$$\frac{d}{dt}(\dot{m}_7) = \left(\frac{A_7}{L_7}\right) [P_G - P_C] \tag{15}$$

$$\frac{d}{dt}(\dot{m}_{10}) = \left(\frac{A_{10}}{L_{10}}\right) [P_E - P_A] \tag{16}$$

$$\frac{1}{2} \xi_1 \frac{1}{\rho_8 A_{V1}^2} \dot{m}_8 |\dot{m}_8| = P_C - P_E \tag{17}$$

$$\frac{1}{2} \xi_2 \frac{1}{\rho_6 A_{V2}^2} \dot{m}_6 |\dot{m}_6| = P_G - P_A \tag{18}$$

where  $\xi_i$  is the expansion valve friction factor considered constant in this research [7–11].  $L_i, d_i,$  and  $A_i$  are the length, diameter, and cross-sectional area of the pipe, respectively.  $\rho_i$  is the density and  $P_i$  is the pressure. The smallest cross sectional area of the expansion valve is indicated by  $A_{Vi}$  [11]. Also, it is assumed that the performance of pump in this cycle is evaluated by the polynomial expression obtained from the characteristic curves (Ref. [9]): Table 1, show the constant coefficients of the polynomial and the expansion valve friction factors.

**Table 1** Constant data are used in dynamic simulation [9]

$\xi_1$	$\xi_2$	$a_1$	$a_2$	$a_3$
0.5	0.5	7.623	128.4	-2941

$$P_G - P_A = a_0 + a_1 \dot{m}_1 + a_2 \dot{m}_1^2 \tag{19}$$

Letting  $h_i(t)$  be the specific enthalpy, the energy balances for the components are given by [8–11]:

$$\frac{d}{dt}(h_C) = \left(\frac{1}{M_C}\right) [\dot{m}_7 h_7 - \dot{m}_8 h_8 - \dot{Q}_C - h_C(\dot{m}_7 - \dot{m}_8)] \tag{20}$$

$$\frac{d}{dt}(h_E) = \left(\frac{1}{M_E}\right) [\dot{m}_8 h_9 - \dot{m}_{10} h_{10} + \dot{Q}_E - h_E(\dot{m}_8 - \dot{m}_{10})] \tag{21}$$

$$\frac{d}{dt}(h_A) = \left(\frac{1}{M_A}\right) [\dot{m}_{10} h_{10} + \dot{m}_6 h_6 - \dot{m}_1 h_1 - \dot{Q}_A - h_A(\dot{m}_{10} + \dot{m}_6 - \dot{m}_1)] \tag{22}$$

$$\frac{d}{dt}(h_G) = \left(\frac{1}{M_G}\right) [\dot{m}_1 h_3 - \dot{m}_6 h_4 - \dot{m}_7 h_7 + \dot{Q}_G - h_G(\dot{m}_1 - \dot{m}_6 - \dot{m}_7)] \tag{23}$$

$$h_5 = h_6 \tag{24}$$

$$h_8 = h_9 \tag{25}$$

$$\dot{Q}_E = \dot{m}_{17} c_p (T_{17} - T_{18}) = UA_E \left[ \frac{(T_{17} - T_E) - (T_{18} - T_9)}{\ln\left(\frac{T_{17} - T_E}{T_{18} - T_9}\right)} \right] \tag{26}$$

$$\dot{Q}_C = \dot{m}_{15} c_p (T_{16} - T_{15}) = UA_C \left[ \frac{(T_C - T_{16}) - (T_C - T_{15})}{\ln\left(\frac{T_C - T_{16}}{T_C - T_{15}}\right)} \right] \tag{27}$$

$$\dot{Q}_A = \dot{m}_{13} c_p (T_{14} - T_{13}) = UA_A \left[ \frac{(T_6 - T_{14}) - (T_A - T_{13})}{\ln\left(\frac{T_6 - T_{14}}{T_A - T_{13}}\right)} \right] \tag{28}$$

$$\dot{Q}_G = \dot{m}_{11} c_p (T_{11} - T_{12}) = UA_G \left[ \frac{(T_{11} - T_G) - (T_{12} - T_7)}{\ln\left(\frac{T_{11} - T_G}{T_{12} - T_7}\right)} \right] \tag{29}$$



where  $UA_i$  is the conductance value for each component [9, 31].

$$COP = \frac{\dot{Q}_E}{\dot{Q}_G} \quad (30)$$

$COP$  is the coefficient of performance of the both ammonia–water and water–lithium bromide absorption cycles [9, 31].

### 3 Solution methods of the modeling

In many studies, the thermodynamic properties of solution were taken from some approximate relations causing the results to be somewhat inaccurate. On the other hand, the EES software is powerful and accurate software in field of thermodynamic issues. In this article to diminish the effect of approximate relations on the results, the Engineering Equation Solver (EES) software is used to define the thermodynamic properties of ammonia–water and water–lithium bromide working fluids. Also, by making a link between MATLAB and EES software the set of differential equations are solved in MATLAB software. The fourth order Runge–Kutta method is employed in solving the differential equations system. Figure 2 shows the basic flowchart of the dynamic model of an absorption chiller.

In this article, each component of the absorption cycle is considered as a control volume and a trial and error process are created for them. The initial values like mass, enthalpy and concentration of main components, the constant values such as temperature and mass flow rate of external water circuit, conductance values and solution heat exchanger's efficiency are given to MATLAB software as input data. Table 2 shows the input values are used in the dynamic model. These values are read by EES software. By using initial values and a hypothetical parameter like pressure, a trial and error process for each component were created in EES software. The pressure variable is considered as a trial and error parameter. Creating a trial and error process was carried out by having initial values such as enthalpy and concentration of the solution at the exit of the generator and hypothetical pressure. Then, generator variables such as temperature, quality and so on, will be obtained. After that, by having these parameters calculate the generator specific volume and will be compared with specific volume that calculating by initial mass. This process is repeated until the convergence criterion is satisfied. Then, the correct values of temperature, pressure and quality of main components are obtained. After that, thermodynamic properties of all points of the cycle and the heat transfer rate of main components are possible to be obtained at each iteration by performing thermodynamic

analysis. The output data such as pressure, mass flow rate at points 1–6–8, the enthalpy of all points of the cycle, concentration of the solution at points 1–6 and heat transfer rate of 4 main components are continuously read in MATLAB software to solve differential equations and the new initial values are obtained. This process is continued until the result reached steady state conditions. Tables 3 and 4 show the initial values used in the dynamic model of aqua-ammonia and water–lithium bromide absorption chillers respectively. To validate dynamic model and determined the initial values, the Herold et al. [31] steady state condition results were used.

### 4 Validation and verification of the dynamic modeling

To validate the dynamic code, the results extracted from numerical simulation of both aqua-ammonia and Water–Lithium bromide absorption cycles are compared with steady state results obtained by Herold et al. [31]. Results obtained from the present dynamic analysis, steady state data [31] and also relative error values are reported in Table 5 and 6. As shown in these Tables, the dynamic results have good agreement with their peers. In fact, maximum relative error in aqua-ammonia absorption chiller generated by the  $\dot{m}_1$  stands at 3.93% while it reaches to 9.2% for  $\dot{m}_6$  in the case of water–lithium bromide absorption chiller.

## 5 Dynamic simulation results

### 5.1 Comparison the start-up time of $NH_3-H_2O$ and $H_2O-LiBr$ AC's key parameters under different working conditions

In this paper, transient behavior of main parameters of aqua-ammonia and water–lithium bromide absorption chillers like  $COP$  and heat transfer rate of the main components under three different cases are compared:

1. Utilizing RHX with SHX in the cycle (both, case A).
2. Removing RHX from the cycle, just SHX plays role in the cycle (Just SHX, case B).
3. Removing SHX from the cycle, just RHX plays role in the cycle (Just RHX, case C).

To be precise, the time that an absorption chiller needs to reach the designed working condition is called start-up. During this time, energy is consumed in the system while efficient refrigeration is not available. So, it's too important to consider the influencing parameters

**Fig. 2** Basic flow chart of the dynamic model of an absorption chiller

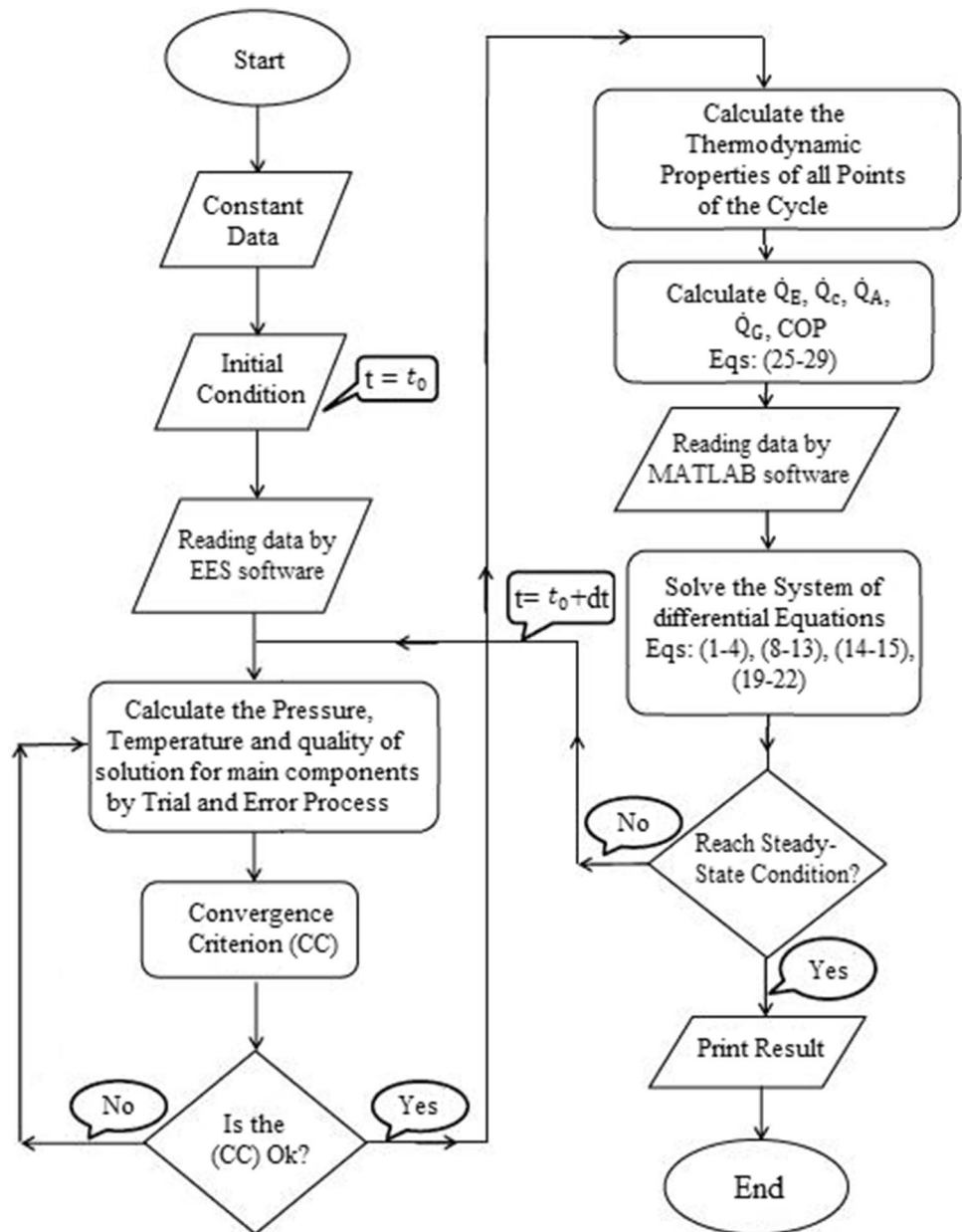


**Table 2** Typical set of input data for the absorption cycle [31]

$\epsilon_{shx}$	$UA_A$ (kW/K)	$UA_G$ (kW/K)	$UA_C$ (kW/K)	$UA_E$ (kW/K)	$\dot{m}_{11}$ (kg/s)	$\dot{m}_{13}$ (kg/s)	$\dot{m}_{15}$ (kg/s)	$\dot{m}_{17}$ (kg/s)	$T_{11}$ (°C)	$T_{13}$ (°C)	$T_{15}$ (°C)	$T_{17}$ (°C)
0.8	1.8	1	1.2	2.25	1	0.28	0.28	0.4	100	25	25	10

**Table 3** Typical set of initial values for the H<sub>2</sub>O–LiBr absorption cycle

$h_A$ (kJ/kg)	$h_C$ (kJ/kg)	$h_E$ (kJ/kg)	$h_G$ (kJ/kg)	$M_A$ (kg)	$M_C$ (kg)	$M_E$ (kg)	$M_G$ (kg)	$Z_G$ (%)	$Z_A$ (%)	$\dot{m}_7$ (kg/s)	$\dot{m}_{10}$ (kg/s)
1282	1020	2060	1290	16	2.26	2.35	15.16	36.7	28.5	0.0043	0.00426

**Table 4** Typical set of initial values for the NH<sub>3</sub>–H<sub>2</sub>O absorption cycle

$h_A$ (kJ/kg)	$h_C$ (kJ/kg)	$h_E$ (kJ/kg)	$h_G$ (kJ/kg)	$M_A$ (kg)	$M_C$ (kg)	$M_E$ (kg)	$M_G$ (kg)	$X_G$ (%)	$X_A$ (%)	$\dot{m}_7$ (kg/s)	$\dot{m}_{10}$ (kg/s)
-40	800	940	370	9	4	4	8	35.5	36	0.1397	0.1388

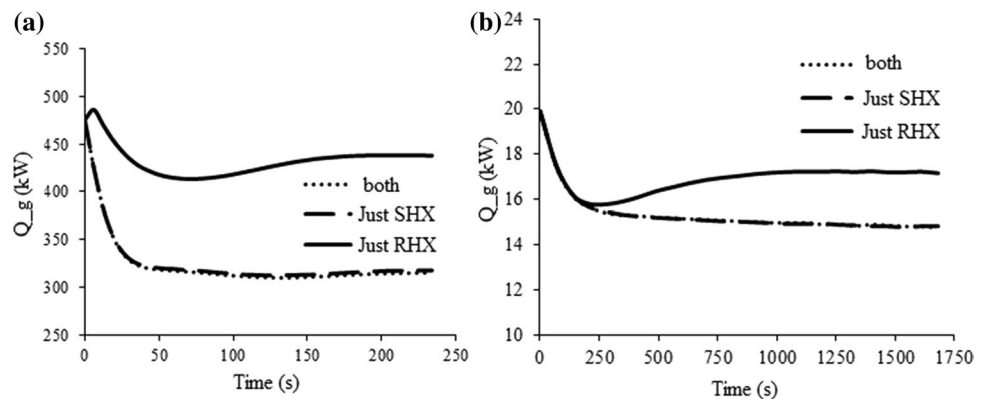
**Table 5** The dynamic simulation result compared to steady state one [31] for H<sub>2</sub>O–LiBr absorption chiller

	COP	$Q_A$ (kW)	$Q_C$ (kW)	$Q_E$ (kW)	$Q_G$ (kW)	$P_G$ (kPa)	$P_E$ (kPa)	$\dot{m}_1$ (kg/s)	$\dot{m}_6$ (kg/s)	$X_A$ (%)	$X_G$ (%)
Ref. [31]	0.724	14.09	11.31	10.67	14.73	7.406	0.676	0.05	0.0454	56.48	62.16
Current study	0.713	14.1	10.78	10.57	14.82	7.44	0.679	0.051	0.05	57.04	61.85
Absolute value of relative error (%)	1.477	0.07	4.686	0.937	0.607	0.456	0.441	1.96	9.2	0.981	0.498

**Table 6** The dynamic simulation result compared to steady state one [31] for NH<sub>3</sub>–H<sub>2</sub>O absorption chiller

	COP	$Q_A$ (kW)	$Q_C$ (kW)	$Q_E$ (kW)	$Q_G$ (kW)	$P_G$ (kPa)	$P_E$ (kPa)	$\dot{m}_1$ (kg/s)	$\dot{m}_6$ (kg/s)	$X_A$ (%)	$X_G$ (%)
Ref. [31]	0.447	273.9	159.2	146.9	327.5	1556	286.4	1	0.857	39.62	29.62
Current study	0.451	279.65	162.5	143.3	317.8	1564	290.4	1.041	0.886	39.53	29.63
Absolute value of relative error (%)	0.886	2.056	2.03	2.45	2.961	0.511	1.377	3.93	3.27	0.227	0.033

**Fig. 3 a** Variation the generator heat transfer rate of the NH<sub>3</sub>–H<sub>2</sub>O AC versus time in 3 different cases. **b** Variation the generator heat transfer rate of the H<sub>2</sub>O–LiBr AC versus time in 3 different cases



on this period of time in order to reduce the energy consumption. Figure 3a, b show the variation of generator’s heat transfer rate for both ammonia–water and water–lithium bromide absorption cycles versus time in three cases mentioned above. The result shows that removing the solution heat exchanger from the cycle (case C) causes 28% and 14% increase in  $Q_G$  of NH<sub>3</sub>–H<sub>2</sub>O and H<sub>2</sub>O–LiBr ACs respectively, happening due to lack of heat transfer from point 4 to 3. Besides, it is found that generator start-up time at aqua-ammonia and water–lithium bromide absorption cycles increases in terms of time by 90 and 250 s respectively. To be precise, the percentage of this increase for NH<sub>3</sub>–H<sub>2</sub>O AC is about 47.36%, and stands at 22.72% in the case of H<sub>2</sub>O–LiBr. Figure 3a, b show that utilizing or removing refrigerant

heat exchanger in both absorption cycles does affect neither  $Q_G$  nor its dynamic response.

As seen in Fig. 3a, at the beginning of the simulation,  $Q_G$  of NH<sub>3</sub>–H<sub>2</sub>O absorption cycle in case C initially increased and after about 15 s decreased. Decrease in the weak solution enthalpy of the generator inlet (lack of heat transfer from point 4–3) and fall in the generator temperature resulted in initially raise in  $Q_G$ . As the time passed by 15 s, the ammonia vapor enthalpy at the absorber inlet is increased by refrigerant heat exchanger, leading to an increase in the absorber temperature as well as weak solution at the generator inlet, and this would itself reduce the  $Q_G$  of the NH<sub>3</sub>–H<sub>2</sub>O AC. Reducing the  $Q_G$  results in reduction in the ammonia vapor generated in the generator, and consequently reduces



the cooling capacity and the enthalpy of the solution at point 3 about 80 s. The  $Q_G$  increases at 80 s and then reaches to steady state condition, shown in Fig. 3a, due to decrease in the enthalpy of the solution at point 3. Figure 3b shows that  $Q_G$  of the water–lithium bromide AC does not change in 3 cases until 250 s. After that, cases A and B reach steady state condition. However, in case C,  $Q_G$  increases after 250 s and reaches steady state condition by 1100 s. This increase has been brought about because of removing the solution heat exchanger from the cycle (lack of heat transfer from point 4 to 3) and reducing the solution enthalpy at point 3.

Variation of  $\text{NH}_3\text{-H}_2\text{O}$  AC condenser heat transfer rate versus time for 3 cases is illustrated in Fig. 4a. At the beginning the simulation, temperature and heat transfer rate of the condenser increases due to the high temperature of the ammonia vapor entering the condenser (temperature difference between condenser chamber and point 9) in all three cases. According to the Fig. 4a,  $Q_c$  in case of C decreases after 40 s, and after 100 s it increases and then reaches steady state condition. The reduction of  $Q_c$  after 40 s is due to the reduction of the ammonia vapor enthalpy at the generator outlet (removing SHX). On the other hand, the refrigerant heat exchanger with regard to liquid enthalpy reduction at the condenser outlet increases the enthalpy of the refrigerant vapor at the absorber inlet and the weak solution enthalpy at the generator inlet as well. Also, increase in enthalpy at point 9 causes an increase in  $Q_c$  after 100 s.

As seen in Fig. 4a, removing SHX from the cycle (case C) causes a reduction in  $\text{NH}_3\text{-H}_2\text{O}$  AC's  $Q_c$  and increases the start-up time from 180 to 210 s. In case C,  $Q_c$  of the  $\text{NH}_3\text{-H}_2\text{O}$  AC increases by 14.28% and has no effect on

$\text{H}_2\text{O-LiBr}$  AC's which is illustrated in Fig. 4a, b. Also, removing RHX from the cycle (case B) has marginal effect on the dynamic response of  $Q_c$  in both absorption cycles. The result shows that the  $Q_c$  of  $\text{NH}_3\text{-H}_2\text{O}$  AC has been highly affected by removing SHX while its effect on  $\text{H}_2\text{O-LiBr}$  AC has been minor.

Variation of evaporator heat transfer rate of  $\text{NH}_3\text{-H}_2\text{O}$  and  $\text{H}_2\text{O-LiBr}$  AC versus time for 3 cases are illustrated in Fig. 5a, b respectively. According to these figures, the use of refrigerant heat exchanger with solution heat exchanger (case A) has significantly increased  $Q_e$  up to 10% in an aqua-ammonia absorption cycle however it has marginal impact on water–lithium bromide cycle. Moreover, increase in  $Q_e$  happens due to reduction of refrigerant enthalpy inside the evaporator and consequently temperature difference reduction between evaporator chamber and chilled water circulation in evaporator. Figure 5a shows that  $Q_e$  of  $\text{NH}_3\text{-H}_2\text{O}$  AC reaches steady state condition near to 200 s in when just SHX is used, and this value stands at 155 s in case of RHX. In fact, employment of SHX accompanied with RHX (case A) means increasing the start-up time of  $Q_e$  of the  $\text{NH}_3\text{-H}_2\text{O}$  AC by 22.5%, not having effect on the dynamic response of the  $\text{H}_2\text{O-LiBr}$  AC evaporator heat transfer rate. The result shows that the evaporator component of  $\text{NH}_3\text{-H}_2\text{O}$  AC has been highly affected by utilizing RHX while it has marginal impact on  $\text{H}_2\text{O-LiBr}$  AC.

Figure 6a, b show the variation of coefficient of performance (COP) versus time for both absorption chillers in different cases. The result represents that utilizing the RHX (case A) causes slight improvement in the COP of the  $\text{NH}_3\text{-H}_2\text{O}$  and  $\text{H}_2\text{O-LiBr}$  AC by 11.16% and 1.8% respectively. Also, solution heat exchanger utilization

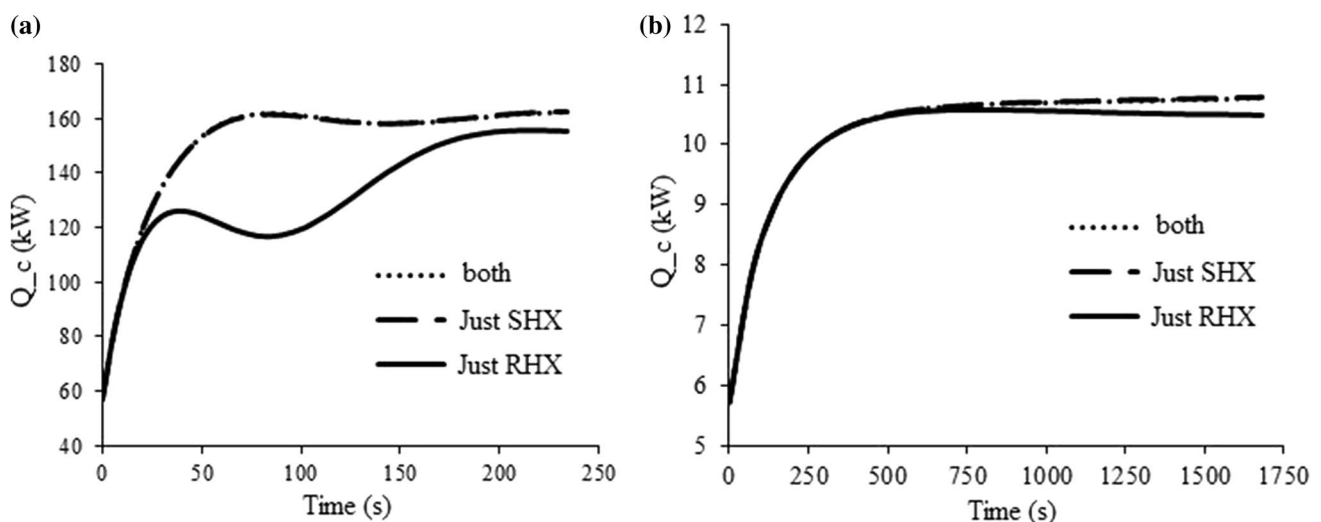


**Fig. 4** **a** Variation of the condenser heat transfer rate of the  $\text{NH}_3\text{-H}_2\text{O}$  AC versus time in 3 different cases. **b** Variation of the condenser heat transfer rate of the  $\text{H}_2\text{O-LiBr}$  AC versus time in 3 different cases

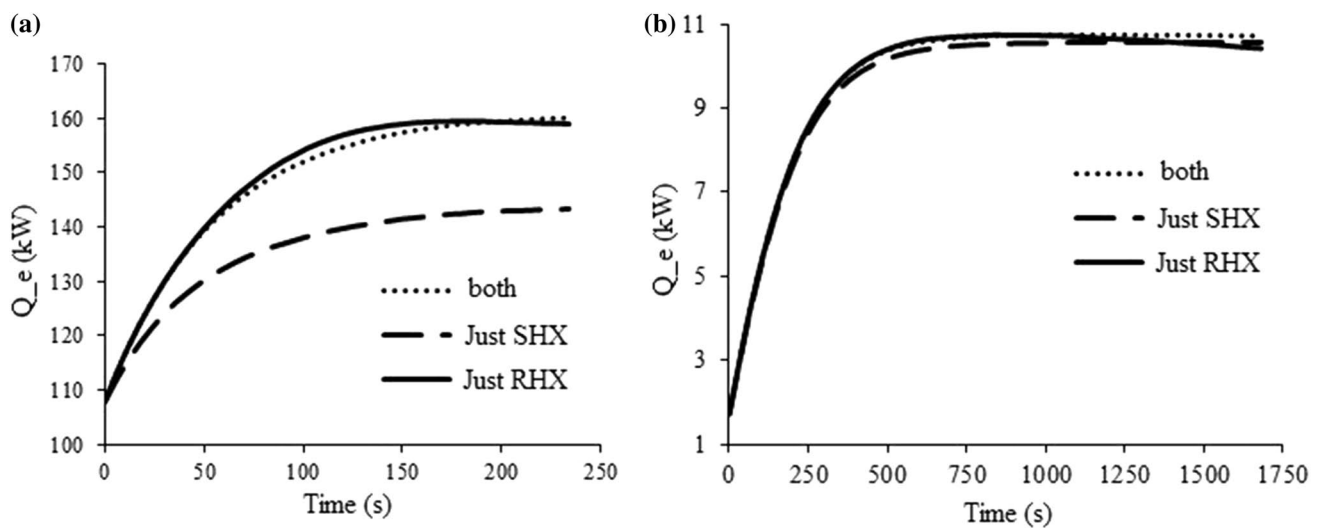


**Fig. 5** **a** Variation of the evaporator heat transfer rate of the  $\text{NH}_3\text{-H}_2\text{O}$  AC versus time in 3 different cases. **b** Variation of the evaporator heat transfer rate of the  $\text{H}_2\text{O-LiBr}$  AC versus time in 3 different cases

with refrigerant heat exchanger increases the  $\text{NH}_3\text{-H}_2\text{O}$  absorption chiller's COP by 28.53%, and this value for  $\text{H}_2\text{O-LiBr}$  stands at only 16.38%. Removing SHX from the cycle (case C) makes the start-up time of the ammonia-water AC's COP experience an increase from 150 s to 170 s, and this value is accordingly counted for water-lithium bromide AC's COP from 850 s to 1550 s. According to Fig. 6a, the  $\text{NH}_3\text{-H}_2\text{O}$  absorption chiller's COP corresponding with (case C) decreases after 80 s and reaches steady state condition at 170 s, happening because of increase in generator thermal load at 80 s. Figure 6b shows the coefficient of performance of the

water-lithium bromide AC does not change through three cases up until 250 s. After that, the COP for cases A and B meets steady state condition. However, the COP decreases after 250 s and reaches steady state condition near to 1250 s in case C. Fall in the COP happens owing to raise in generator heat transfer rate after 250 s.

The result shows that the influence of utilizing the RHX is only imposed on the evaporator thermal load and the COP, and does not affect the dynamic response of the different parameters of the both absorption chillers. In this regard, the  $\text{NH}_3\text{-H}_2\text{O}$  absorption cycle has been highly affected in comparison with the  $\text{H}_2\text{O-LiBr}$  AC. The

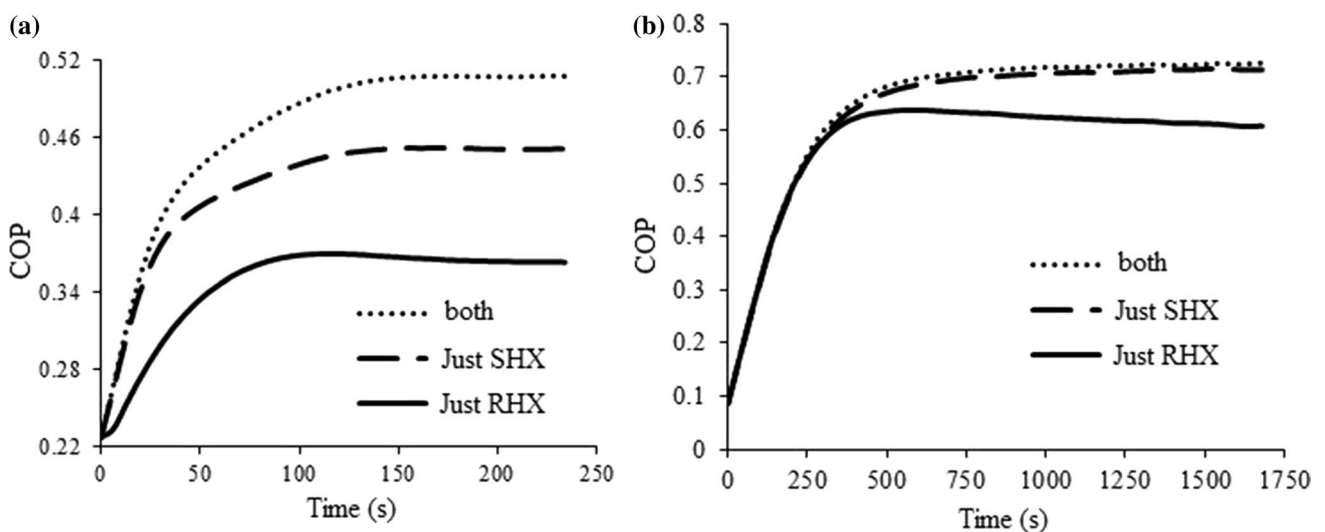


**Fig. 6** **a** Variation of the COP of the  $\text{NH}_3\text{-H}_2\text{O}$  AC versus time in 3 different cases. **b** Variation of the COP of the  $\text{H}_2\text{O-LiBr}$  AC versus time in 3 different cases

importance of using SHX for both absorption cycles is much greater than the RHX. According to the result, the start-up time of various parameters of water–lithium bromide absorption chiller is highly affected in comparison with the ammonia–water absorption cycle. Then, removing the SHX from the cycle leads to increase in start-up time of the coefficient of performance of the  $\text{NH}_3\text{-H}_2\text{O}$  AC by 11.76%, and this value is counted as 45.16% in which case the  $\text{H}_2\text{O-LiBr}$  absorption chiller is used.

## 5.2 Comparison the effect of solution heat exchanger's efficiency on the start-up time of the key parameters of both ACs

As already mentioned, heat exchanger's components play a very important role in the absorption cycles. Also, the heat exchanger's efficiency has significant impact in the absorption cycle. In this section, the effect of solution heat exchanger's efficiency on start-up time of the key parameters of the both AC is discussed and compared. Figure 7a, b indicate the variation of coefficient of performance (COP) versus time for both absorption chillers in different SHX efficiencies. It can be concluded from these figures that increase in SHX efficiency results in COP enhancement for both absorption cycles and this happens owing to reduction in the generator heat transfer rate. In addition, it is revealed that in which case the efficiency of solution heat exchanger goes up from 0.55 to 0.8, COP of the  $\text{NH}_3\text{-H}_2\text{O}$  absorption cycle increases from 0.388 to 0.451, which means 13.92% enhancement. And in case of  $\text{H}_2\text{O-LiBr}$  AC, COP ranges from 0.6909 to 0.764 and accordingly brings 9.7% profit. Also, the start-up time of the COP related to  $\text{NH}_3\text{-H}_2\text{O}$  AC increases 9.6%, and this value stands at

46.42% in case  $\text{H}_2\text{O-LiBr}$  AC is used. According to Fig. 7a, COP of the  $\text{NH}_3\text{-H}_2\text{O}$  absorption chiller corresponding with 0.55 SHX efficiency decreases after 100 s and then reaches steady state condition, happening due to reduction in generator heat transfer rate at a certain time. By increasing the SHX efficiency (decrease in generator heat transfer rate), intensity of this reduction decreases and at a certain SHX efficiency ( $\epsilon = 0.8$ ), COP increases. Figure 7a, b reported that in  $\text{H}_2\text{O-LiBr}$  AC, SHX efficiency enhancement has slightly influenced the COP by 9.7% but has applied a valuable increase in the COP start-up time around 11 min. In contrast, SHX efficiency enhancement in  $\text{NH}_3\text{-H}_2\text{O}$  AC, has a minor impact on COP start-up time (near to 15 s) while remarkably influences the COP by 14%.

## 6 Discussion

Nowadays, due to the unceasing increase in electric energy consumption, the rising cost of fuel and destructive effects of the HCFC refrigerant on the ozone layer and the global warming problem, absorption chillers are more considered. The time required an absorption chiller achieves its design condition is called Start-up time and during this time, energy is used however the effective refrigeration wouldn't be achieved. Also, dynamic analysis can be used to reduce the startup time and increase system performance in addition to strategic control purposes. Optimizing the absorption cycle during transient operations, such as start up or shut down is of interests. In this article, in order to mitigate the effect of approximate relations on the outcomes, the thermodynamic properties of  $\text{NH}_3\text{-H}_2\text{O}$  and  $\text{H}_2\text{O-LiBr}$  solutions are extracted from the

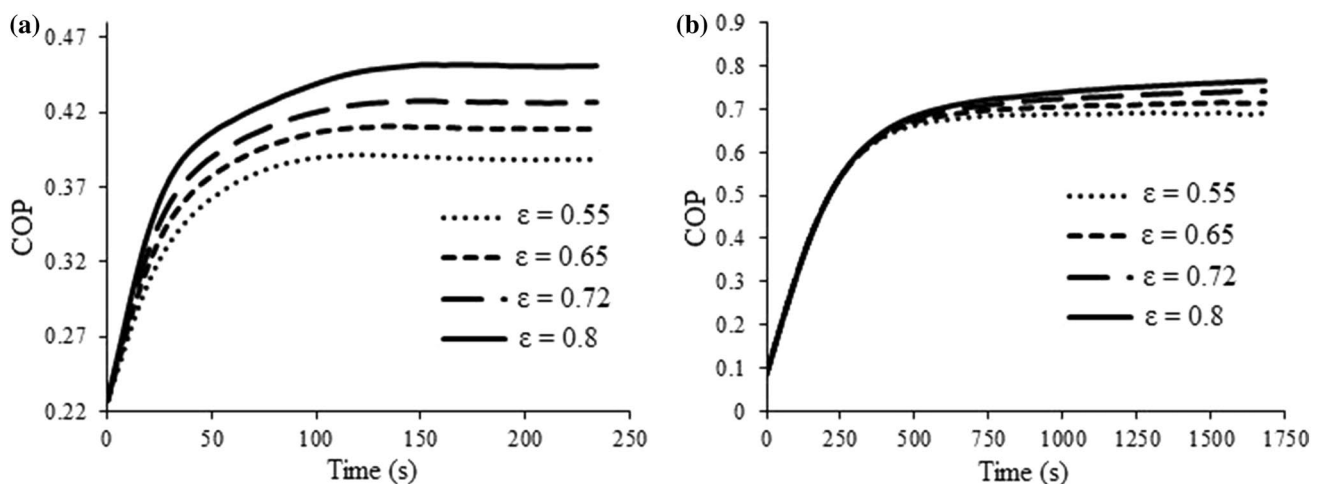


**Fig. 7** **a** Variation of the COP of the  $\text{NH}_3\text{-H}_2\text{O}$  AC versus time at different SHX efficiency. **b** Variation of the COP of the  $\text{H}_2\text{O-LiBr}$  AC versus time at different SHX efficiency

EES software. By making a link between MATLAB and EES software, a set of differential equations is solved in MATLAB software. This study deals with a lumped-parameters dynamic simulation of aqua-ammonia and water–lithium bromide absorption chillers under three different conditions including, (1) utilizing RHX within SHX in the cycle, (2) removing RHX from the cycle, just SHX plays the role in the cycle and (3) removing SHX from the cycle, just RHX plays the role in the cycle. The effect of employing refrigerant and solution heat exchangers and solution heat exchanger's efficiency on the start-up time of the key parameters of both ACs studied and compared.

Many researches have been carried out through steady state condition to analyze the absorption chiller's performance. The results in literature show that employing SHX in absorption chillers and increasing the effectiveness of the SHX has caused generator heat load decrement in addition to an increase in COP [22, 23, 33]. Also, employing SHX in ACs grows up the COP more than 44% while this value for RHX stands at only 2.8% [22, 33]. Based on researchers' findings, the absorption chillers performance is highly affected by SHX in comparison with RHX [22, 23, 33]. Our dynamic simulation outcomes represent that utilizing the RHX causes slight improvement in COP value of both  $\text{NH}_3\text{-H}_2\text{O}$  and  $\text{H}_2\text{O-LiBr}$  ACs by 11.16% and 1.8%, respectively. Also, the use of SHX increases the COP of  $\text{NH}_3\text{-H}_2\text{O}$  absorption chiller by 28.53%, and this value for  $\text{H}_2\text{O-LiBr}$  stands at only 16.38%. Removing solution heat exchanger from the cycle increases the start-up time of COP of the  $\text{NH}_3\text{-H}_2\text{O}$  and  $\text{H}_2\text{O-LiBr}$  ACs by 11.76% and 45.16% respectively. According to the results, by increasing the SHX efficiency from 0.55 to 0.8, the COP of the  $\text{NH}_3\text{-H}_2\text{O}$  and  $\text{H}_2\text{O-LiBr}$  ACs increases by 13.92% and 9.7%, respectively. Furthermore, the start-up time of the COP related to  $\text{NH}_3\text{-H}_2\text{O}$  AC increases 9.6%, and this value stands at 46.42% in case of  $\text{H}_2\text{O-LiBr}$  AC. In case of  $\text{H}_2\text{O-LiBr}$  AC, increase in SHX efficiency has slightly affected the COP by 9.7%, but it significantly increases the COP start-up time near to 11 min. On the contrary, SHX efficiency enhancement in  $\text{NH}_3\text{-H}_2\text{O}$  AC has minor effect on COP start-up time near to 15 s, having highly affected the COP by 14%.

Our dynamic results represent that the start-up time of the COP of water–lithium bromide absorption chiller is highly affected in comparison with ammonia–water absorption cycle, by removing SHX or increasing the SHX efficiency. Also, by utilizing the RHX does not affect the dynamic response of the key parameters of the both absorption chillers. The importance of using SHX for both absorption cycles is much greater than the RHX.

## 7 Conclusion

Simulations are way very important tools for researchers to predict the performance of absorption chillers at the dynamic level with low cost. Also, dynamic analysis can be used to reduce the startup time and increase system performance in addition to strategic control purposes. The aim of this study was to evaluate and compare the dynamic performance of aqua-ammonia and water–lithium bromide absorption chillers under three different conditions including, (1) utilizing RHX within SHX in the cycle, (2) removing RHX from the cycle, just SHX plays the role in the cycle and (3) removing SHX from the cycle, just RHX plays the role in the cycle. In addition, the impact of solution heat exchanger's efficiency on the start-up time of the key parameters of both ACs was studied. In order to minimize the deviations resulted from approximated equations, the Engineering Equation Solver (EES) software was used to obtain the thermodynamic properties of aqua-ammonia and water–lithium bromide working fluids, and MATLAB software was employed to solve differential equations. To validate the dynamic model, the results extracted from numerical simulations of both aqua-ammonia and water–lithium bromide absorption cycles were compared with steady state results, and relative errors were also reported. The following results were obtained from the dynamic analysis of the cases mentioned above:

1. Removing SHX increases the start-up time of  $Q_g$  of the  $\text{NH}_3\text{-H}_2\text{O}$  and  $\text{H}_2\text{O-LiBr}$  ACs by 47.36% and 22.72% respectively.
2. Removing SHX increases the start-up time of  $Q_c$  of the  $\text{NH}_3\text{-H}_2\text{O}$  AC by 14.28% while it has no effect on  $\text{H}_2\text{O-LiBr}$  AC.
3. Removing SHX increases the start-up time of COP of the  $\text{NH}_3\text{-H}_2\text{O}$  and  $\text{H}_2\text{O-LiBr}$  ACs by 11.76% and 45.16% respectively.
4. In case of  $\text{H}_2\text{O-LiBr}$  AC, increase in SHX efficiency has slightly affected the COP by 9.7%, but it significantly increases the COP start-up time near to 11 min. On the contrary, SHX efficiency enhancement in  $\text{NH}_3\text{-H}_2\text{O}$  AC has minor effect on COP start-up time near to 15 s, having highly affected the COP by 14%.
5. Key parameters of  $\text{H}_2\text{O-LiBr}$  AC in terms of start-up and  $\text{NH}_3\text{-H}_2\text{O}$  AC in terms of quantity are highly affected by removing SHX and increasing the SHX efficiency respectively.

Dynamic simulation of triple-stage absorption chiller by HYSYS software, analysis and economic optimization of triple-stage absorption chillers, and new controller design



to reduce the absorption chiller energy consumption are suggested as a future research.

## Compliance with ethical standards

**Conflict of interest** The authors declare that they have no conflict of interest.

## References

1. Chua HT et al (2000) A general thermodynamic framework for understanding the behavior of absorption chillers. *Int J Refrig* 23(7):491–507. [https://doi.org/10.1016/S0140-7007\(99\)00077-8](https://doi.org/10.1016/S0140-7007(99)00077-8)
2. Lee S-F, Sherif SA (2001) Thermodynamic analysis of a lithium bromide/water absorption system for cooling and heating applications. *Int J Energy Res* 25(11):1019–1031. <https://doi.org/10.1002/er.738>
3. Yang M et al (2017) High efficiency H<sub>2</sub>O/LiBr double effect absorption cycles with multi-heat sources for tri-generation application. *Appl Energy* 187:243–254. <https://doi.org/10.1016/j.apenergy.2016.11.067>
4. Lake A, Rezaie B, Beyerlein S (2017) Use of exergy analysis to quantify the effect of lithium bromide concentration in an absorption chiller. *Entropy* 19(4):156. <https://doi.org/10.3390/e19040156>
5. Kohlenbach P, Ziegler F (2008) A dynamic simulation model for transient absorption chiller performance. Part I: the model. *Int J Refrig* 31(2):217–225. <https://doi.org/10.1016/j.ijrefrig.2007.06.009>
6. Kohlenbach P, Ziegler F (2008) A dynamic simulation model for transient absorption chiller performance. Part II: numerical results and experimental verification. *Int J Refrig* 31(2):226–233. <https://doi.org/10.1016/j.ijrefrig.2007.06.010>
7. Kim Byongjoo, Park Jongil (2007) Dynamic simulation of a single-effect ammonia–water absorption chiller. *Int J Refrig* 30:535–545. <https://doi.org/10.1016/j.ijrefrig.2006.07.004>
8. Cai Weihua, Sen Mihir, Paolucci Samuel (2010) Dynamic simulation of an ammonia–water absorption refrigeration system. *Ind Eng Chem Res* 51:2070–2076. <https://doi.org/10.1021/ie200673f>
9. Iranmanesh A, Mehrabian M (2013) Dynamic simulation of a single-effect H<sub>2</sub>O–LiBr absorption refrigeration cycle considering the effects of thermal masses. *Energy Build* 60:47–59. <https://doi.org/10.1016/j.enbuild.2012.12.015>
10. Cerezo J et al (2018) Dynamic simulation of an absorption cooling system with different working mixtures. *Energies* 11(2):259. <https://doi.org/10.3390/en11020259>
11. Ebrahimnataj Tiji A, Ramiar A, Ebrahimnataj MR (2019) Investigation of the launch time of NH<sub>3</sub>–H<sub>2</sub>O absorption chiller under different working condition. *Proc Inst Mech Eng Part E J Process Mech Eng*. <https://doi.org/10.1177/0954408919879871>
12. Wang J et al (2017) Dynamic performance analysis for an absorption chiller under different working conditions. *Appl Sci* 7(8):797. <https://doi.org/10.3390/app7080797>
13. Shin Y, Seo JA, Cho HW, Nam SC, Jeong JH (2009) Simulation of dynamics and control of a double-effect LiBr–H<sub>2</sub>O absorption chiller. *Appl Therm Eng* 29(13):2718–2725. <https://doi.org/10.1016/j.applthermaleng.2009.01.006>
14. Viswanathan VK, Rattner AS, Determan MD, Garimella S (2012) Dynamic model for a small-capacity ammonia–water absorption chiller. *HVAC&R Res* 19:865–881. <https://doi.org/10.1080/10789669.2013.833974>
15. Fu DG, Poncia G, Lu Z (2006) Implementation of an object-oriented dynamic modeling library for absorption refrigeration systems. *Appl Therm Eng* 26(2–3):217–225. <https://doi.org/10.1016/j.applthermaleng.2005.05.008>
16. Dence AE, Nowak CC, Perez-Blanco H (1996) A transient computer simulation of an ammonia–water heat pump in cooling mode. In: *Energy conversion engineering conference*, pp 1041–1046. <https://doi.org/10.1109/ieccc.1996.553843>
17. Jeong S, Kang BH, Karng SW (1998) Dynamic simulation of an absorption heat pump for recovering low grade waste heat. *Appl Therm Eng* 18:1–12. [https://doi.org/10.1016/S1359-4311\(97\)00040-9](https://doi.org/10.1016/S1359-4311(97)00040-9)
18. Kaushik SC, Rao SK, Kumari R (1991) Dynamic simulation of an aqua-ammonia absorption cooling system with refrigerant storage. *Energy Convers Manag* 32(3):197–206. [https://doi.org/10.1016/0196-8904\(91\)90123-Z](https://doi.org/10.1016/0196-8904(91)90123-Z)
19. Mbikan M, Al-Shemmeri T (2017) Computational model of a biomass driven absorption refrigeration system. *Energies* 10(2):234. <https://doi.org/10.3390/en10020234>
20. Altun AF, Kilic M (2020) Economic feasibility analysis with the parametric dynamic simulation of a single effect solar absorption cooling system for various climatic regions in Turkey. *Renew Energy*. <https://doi.org/10.1016/j.renene.2020.01.055>
21. Wang X et al (2020) Dynamic performance comparison of different cascade waste heat recovery systems for internal combustion engine in combined cooling, heating and power. *Appl Energy* 260:114245. <https://doi.org/10.1016/j.apenergy.2019.114245>
22. Kaushik SC, Arora A (2009) Energy and exergy analysis of single effect and series flow double effect water–lithium bromide absorption refrigeration systems. *Int J Refrig* 32(6):1247–1258. <https://doi.org/10.1016/j.ijrefrig.2009.01.017>
23. Sözen Adnan (2001) Effect of heat exchangers on performance of absorption refrigeration systems. *Energy Convers Manag* 42(14):1699–1716. [https://doi.org/10.1016/S0196-8904\(00\)00151-5](https://doi.org/10.1016/S0196-8904(00)00151-5)
24. Kaynakli Omer, Kilic Muhsin (2007) Theoretical study on the effect of operating conditions on performance of absorption refrigeration system. *Energy Convers Manag* 48(2):599–607. <https://doi.org/10.1016/j.enconman.2006.06.005>
25. Karamangil MI, Coskun S, Kaynakli O, Yamankaradeniz N (2010) A simulation study of performance evaluation of single-stage absorption refrigeration system using conventional working fluids and alternatives. *Renew Sustain Energy Rev* 14(7):1969–1978. <https://doi.org/10.1016/j.rser.2010.04.008>
26. Samutr P, Alili AA (2016) A dynamic model of a single-stage LiBr–H<sub>2</sub>O absorption chiller. *Energy Sustain*. <https://doi.org/10.1115/es2016-59383>
27. Ochoa AAV et al (2016) Dynamic study of a single effect absorption chiller using the pair LiBr/H<sub>2</sub>O. *Energy Convers Manag* 108:30–42. <https://doi.org/10.1016/j.enconman.2015.11.009>
28. Ochoa AAV et al (2017) The influence of the overall heat transfer coefficients in the dynamic behavior of a single effect absorption chiller using the pair LiBr/H<sub>2</sub>O. *Energy Convers Manag* 136:270–282. <https://doi.org/10.1016/j.enconman.2017.01.020>
29. Kerme ED et al (2017) Energetic and exergetic analysis of solar-powered lithium bromide–water absorption cooling system. *J Clean Prod* 151:60–73. <https://doi.org/10.1016/j.jclepro.2017.03.060>
30. Mansouri Rami, Bourouis Mahmoud, Bellagi Ahmed (2018) Steady state investigations of a commercial diffusion-absorption refrigerator: experimental study and numerical simulations. *Appl Therm Eng* 129:725–734. <https://doi.org/10.1016/j.applthermaleng.2017.10.010>
31. Herold KE, Radermacher R, Klein SA (2016) *Absorption chillers and heat pumps*, 2nd edn. CRC Press Inc., Boca Raton



32. Yuwardi Y (2013) Absorption cooling in district heating network: temperature difference examination in hot water circuit. MSc thesis, KTH, School of Industrial Engineering and Management (ITM)
33. Aphornratana S, Sriveerakul T (2007) Experimental studies of a single-effect absorption refrigerator using aqueous lithium-bromide: effect of operating condition to system performance.

Exp Therm Fluid Sci 32(2):658–669. <https://doi.org/10.1016/j.expthermflusci.2007.08.003>

**Publisher's Note** Springer Nature remains neutral with regard to jurisdictional claims in published maps and institutional affiliations.